NONRECIPROCAL MILLIMETER WAVE PROPAGATION IN SLOT GUIDING STRUCTURES USING MAGNETOPLASMONS*

Clifford M. Krowne,† Ayman A. Mostafa,** Kawthar A. Zaki**

†Electronics Science and Technology Division, Naval Research Laboratory
Washington, D.C. 20375-5000.

**University of Maryland, Department of Electrical Engineering
College Park, Maryland 20742.

ABSTRACT

A full wave spectral domain approach for general anisotropy is used to determine the nonreciprocal phase and attenuation properties of slot line structures. Dominant mode dispersive behavior is controlled by the semiconductor substrate characteristics, geometric dimensions, and magnetic field bias magnitude and angle in the Voigt configuration. Numerical results are presented to establish the nonreciprocal properties up to 85 GHz.

1. INTRODUCTION

Here we provide a study of nonreciprocity in slot planar structures compatible with millimeter wave integrated circuit technology. The approach uses a semiconductor to provide a carrier plasma which is then subjected to a static magnetic field $\vec{B}_0$. The resulting nondiagonalized form of the semiconductor macroscopic tensor $\hat{\epsilon}$ and the field displacement effect [1] lead to different propagation constants γ in the forward γ^+ and reverse γ^- directions. These unequal γ's may contain unequal phase propagation constants (β^+ and β^-) and attenuation constants (α^+ and α^-). Therefore, both β's and α's are studied to find their absolute values and differences $\Delta\alpha = \alpha^+ - \alpha^-$ and $\Delta\beta = \beta^+ - \beta^-$ as functions of ϕ, B_0, T and geometric dimensions. Here ϕ and T are, respectively, the angle of the field in relation to the planar interfaces (inclination angle) and the ambient lattice temperature.

Unlike the large number of studies done in the past using the Faraday configuration which requires polarizers to obtain isolator action based upon $\Delta\alpha = 0$, here the focus is entirely on the use of the Voigt configuration where $\vec{B}_0$ is perpendicular to the direction of propagation. Several recent theoretical investigations [2-5] employing the Voigt configuration have examined open, infinite-in-extent layered structures, propagating surface waves guided by the dielectric-semiconductor interfaces. The frequency range was from several hundred GHz up to a maximum between 700 and 1100 GHz. Semiconductor material utilized was GaAs at 77 K and 10^{15} cm^{-3} n-type doping, implying a particular scattering momentum relaxation time τ_p. Many branches were found for the structures with B_0 in one orientation, namely parallel to the planar layers ($\phi = 0^o$) $-$ B_0 had been set to $\approx$ 3800 G. An attempt to direct attention toward the millimeter wave frequency regime was made more recently by another study which treated a semiconductor loaded waveguide structure [6]. This work considered Si and GaAs semiconductors, B_0 fields up to 10 kG, and several doping densities. Again the Voigt configuration was considered (with $\phi = 0^o$). The theoretical analysis used a few waveguide modes. Both theory and experiment had been done at 92 GHz.

*Work supported in part by NRL contract no. N00014-86K-2013

2. MAGNETOPLASMA PERMITTIVITY TENSOR

In this paper the issue of non-reciprocal guided wave propagation in slot structures for MMIC's is addressed. The structures are covered and have electric side walls normal to the layers. All conductors are assumed perfect. A full wave analysis is used which can handle very general linear macroscopic tensors for the layers [7,8]. Here the anisotropy is restricted to the semiconductor ($\hat{\epsilon}$). A Drude model is employed to describe the individual electron motion in the semiconductor by

$$m^* \frac{d\vec{v}}{dt} = q\,(\vec{E} + \vec{v} \times \vec{B}) - \frac{m^*\vec{v}}{\tau_p} \tag{1}$$

where q, m^*, and τ_p are respectively the electron charge, effective mass, and momentum relaxation time. Electron velocity $\vec{v}$, and fields $\vec{E}$ and $\vec{B}$ include the dc and rf components. Electron particle current density is

$$\vec{J} = q\,n\,\vec{v} \tag{2}$$

with n being the electron density. Expressing all variables Q as

$$Q = Q_0 + Q_{rf}\, e^{j\omega t - \gamma z}, \tag{3}$$

letting $|\vec{B}_0| >> |\vec{B}_{rf}|$, and extracting out of (1) and (2) the first order perturbation, allows resistivity in

$$\vec{E}_{rf} = \hat{\rho}\vec{J}_{rf} \tag{4}$$

to be determined as

$$\hat{\rho} = \begin{bmatrix} j\omega + \tau_p^{-1} & 0 & \omega_c \sin\phi \\ 0 & j\omega + \tau_p^{-1} & -\omega_c \cos\phi \\ -\omega_c \sin\phi & \omega_c \cos\phi & j\omega + \tau_p^{-1} \end{bmatrix} \frac{1}{\epsilon\omega_p^2}. \tag{5}$$

Here ϵ is the static permittivity, and ω, ω_p, and ω_c are, respectively, the electromagnetic, plasma, and cyclotron radian frequencies.

$$\omega_p^2 = \frac{qn}{m^*\epsilon} \quad ; \quad \omega_c = \frac{qB_0}{m^*}. \tag{6}$$

0149-645X/88/0000-0211$01.00 © 1988 IEEE

The requirement of a sourceless field problem and a single 6 × 6 constitutive tensor $\hat{M}$ relating $\vec{E}_{rf}$, $\vec{D}_{rf}$, $\vec{H}_{rf}$, and $\vec{B}_{rf}$ [7] leads to permeability $\hat{\mu} = I\mu_0$, optical activities $\hat{\rho}_o = \hat{\rho}_o{}' = 0$ and permittivity

$$\hat{\epsilon} = \epsilon I + \frac{\hat{\sigma}}{j\omega}; \quad \hat{\sigma} = \hat{\rho}^{-1}. \tag{7}$$

For GaAs, Γ electron valley effective masses are appropriate to use so that

$$\omega_c = 2.63 \times 10^{11} B_0 (10^3 kG); \omega_p = 1.93 \times 10^{13} \sqrt{n(10^{17}/cc)}. \tag{8}$$

Attenuation arises from the finite value of the momentum relaxation time τ_p in (5). The off-diagonally $\hat{\rho}$ elements cause $\Delta\alpha$ and $\Delta\beta$ to be non-zero for finite B_0.

3. SLOT ADMITTANCE DYADIC

An admittance-type dyadic Green's function, in the spectral domain, is used to relate surface current $\tilde{\mathbf{J}}$ to tangential electric field $\tilde{\mathbf{E}}$ at the conductor-slot interface.

$$\tilde{J}_x(n) = \tilde{G}'_{11}(\gamma, n)\tilde{E}_x(n) + \tilde{G}'_{12}(\gamma, n)\tilde{E}_z(n) \tag{9a}$$

$$\tilde{J}_z(n) = \tilde{G}'_{21}(\gamma, n)\tilde{E}_x(n) + \tilde{G}'_{22}(\gamma, n)\tilde{E}_z(n). \tag{9b}$$

Dyadic $G' = G^{-1}$, G being the impedance dyadic [8]. Slot electric field components are expanded in terms of complete trigonometric basis function sets satisfying the edge condition. For single slot even and odd modes, we use respectively the basis functions

$$RE_{\substack{x_m \\ z}} = \begin{matrix}\sin \\ \cos\end{matrix} \left\{(2m-1)\frac{\pi x}{w}\right\} \tag{10a}$$

$$RE_{xm}(x) = \cos\left[(m-1)\frac{2\pi x}{w}\right]; \; RE_{zm}(x) = \sin\left[\frac{2\pi x m}{w}\right] \tag{10b}$$

for $|x| \leq w/2$ with $m = 1, 2, \ldots,$ and $R = [1 - (2x/w)^2]^{1/2}$, and the right-hand-sides of (10) are zero otherwise. By taking the finite Fourier transform of (10) according to

$$\tilde{f}(\alpha_n, y) = \int_{-b/2}^{b/2} f(x, y)\, e^{-j\alpha_n x} dx \tag{11}$$

(y = interface; $\alpha_n = (2n-1)\pi/b$ or $2n\pi/b$ for even or odd modes respectively where n = any integer), inserting the result into (9), applying Parseval's theorem, and using a Galerkin approach, a determinantal equation for the propagation constant can be written based on the fact that the slot electric field expansion coefficients are not a trivial null set. Numerical results below are found by setting maximum x and z field expansion indices m to 1 with maximum $n \approx 10^2$ (larger m values have been tested to assure solution convergence).

4. NUMERICAL RESULTS

Figure 1 shows a sketch of a possible slot line (finline) structure. Electromagnetic propagation is either in the z-direction, out

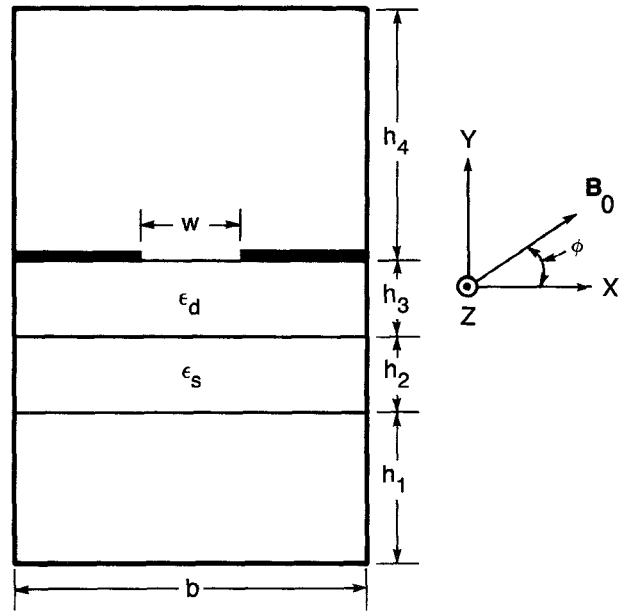

Fig. 1 Cross-section of a slotline structure. Magnetic field B_0 is at inclination angle ϕ to planar surfaces.

of the paper ("+" or forward direction) or into the paper ("-" or reverse direction). The suspended single slot line rests on two substrates, a dielectric with relative permittivity $\epsilon_d = 12.5$ and the semiconductor with $\epsilon_s = \epsilon_d$. Regions of thickness h_1 and h_4 are air (relative permittivity $\epsilon_{r1} = \epsilon_{r4} = 1$, relative permeability $\mu_r = 1$). Slot width $w = 1.0$ mm, and the other geometric dimensions are $b = 2.35$ mm, $h_1 = h_4 = 2.1$ mm, and $h_2 = 0.25$ mm. Thickness h_3 is varied. Numerical results are first presented for $\phi = 0°$, with $\omega_c = 3.14 \times 10^{12}$ rad/sec ($B_0 = 12$ kG), $\omega_p = 6.28 \times 10^{12}$ rad/sec ($n = 10^{16}/cc$), and $\tau_p = 10^{-13}$ sec (room temperature operation). Only the dominant mode is calculated and discussed here. This mode is odd with respect to E_z and even with respect to E_x. In the $B_0 \to 0$ limit, the regular dominant slot line mode is obtained. Figure 2 shows α (dB/mm) (with $\alpha = \alpha^+$ or α^-) versus frequency f (GHz) between 45 and 85 GHz for $h_3 = 0.25$ mm. At the α peaks, $\Delta\alpha/\alpha \approx 15\%$. Normalized phase propagation constant $\bar{\beta} = \beta/\beta_0$ with $\beta = \beta^+$ or β^-, $\beta_0 =$ free space value, is shown in Figs. 3(a) and (b) for respectively $h_3 = 0.25$ mm and $h_3 = 0$ mm. It is evident that $\Delta\bar{\beta}$ increases with decreasing h_3 by comparing Figs. 3(a) and (b). Such behavior is physically understandable since h_3 reduction places the magnetoplasma layer in closer proximity to the slot. $\Delta\bar{\beta}/\bar{\beta} \approx 1.3\%$ across the 45 through 80 GHz frequency range displayed ($h_3 = 0$). Figures 4 and 5 plot, respectively, $\Delta\alpha$ and $\Delta\beta$ versus f between 45 and 75 GHz for h_3 parameterized, $h_3 = 0$, 0.01, 0.1, and 0.25 mm. At the low end of the frequency range in Fig. 5, attenuation difference $\Delta\alpha$ monotonically decreases with rising h_3. However, this is not the situation beyond about 47.7 GHz.

For $f = 75$ GHz, Figs. 6 and 7 show α and $\bar{\beta}$ under varying ϕ. Notice the monotonic decrease of $\Delta\alpha$ and $\Delta\bar{\beta}$ with increasing ϕ, and $\alpha^+ > \alpha^-$ and $\bar{\beta}^+ > \bar{\beta}^-$. For the choice of parameters selected, $\Delta\alpha$, $\Delta\bar{\beta}$, α^-, $\bar{\beta}^+$ and $\bar{\beta}^-$ are all roughly constant up to 15° inclination angle. Attenuation constant α^+ hardly varies (compared to α^-) up to $\phi = 60°$. As $\phi \to 90°$, both $\Delta\alpha$ and $\Delta\beta$

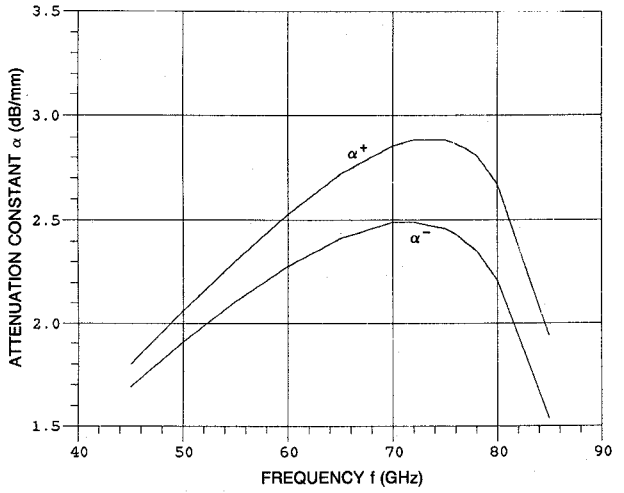

Fig. 2 Dispersion behavior of α^+ and α^-. $B_0 = 12$ kG, $\phi = 0°$, $n = 10^{16}$/cc, $w = 1.0$ mm, and $h_3 = 0.25$ mm.

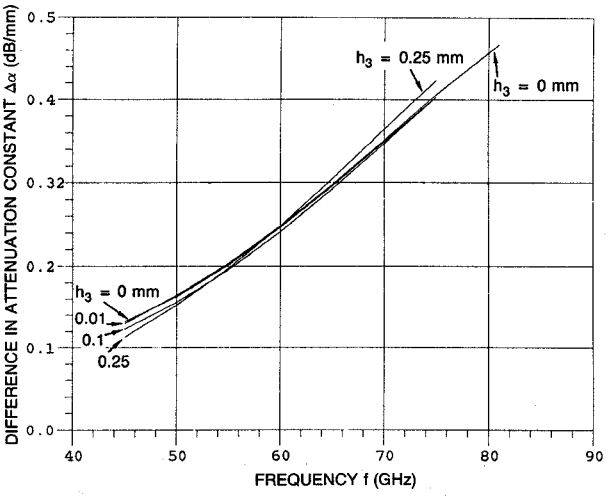

Fig. 4 Dispersion behavior of $\Delta\alpha$, with h_3 parameterized.

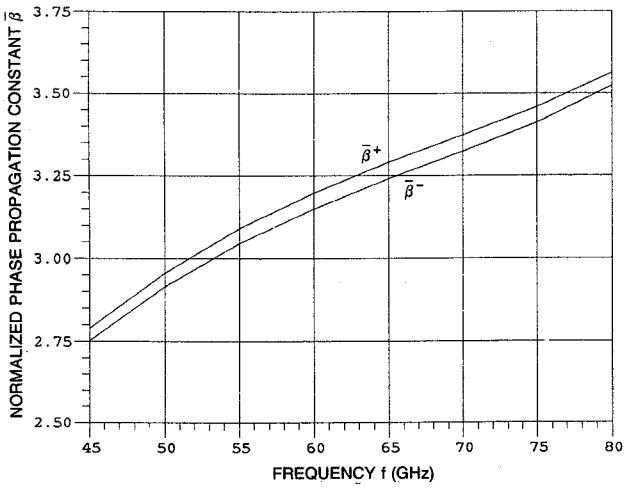

Fig. 3(a) Dispersion behavior of $\bar{\beta}^+$ and $\bar{\beta}^-$. Parameters are the same as in Fig. 2.

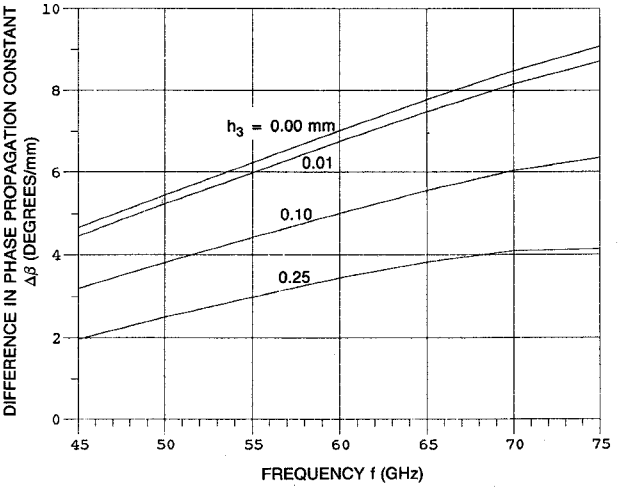

Fig. 5 Dispersion behavior of $\Delta\beta$, with h_3 parameterized.

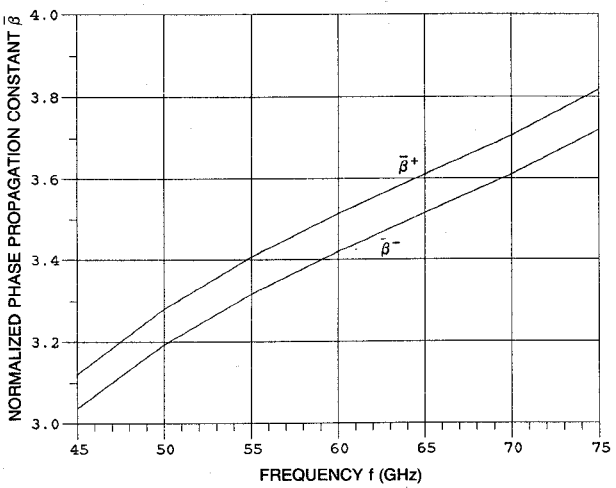

Fig. 3(b) Dispersion behavior of $\bar{\beta}^+$ and $\bar{\beta}^-$. Parameters are as in Fig. 3(a) except $h_3 = 0$ mm.

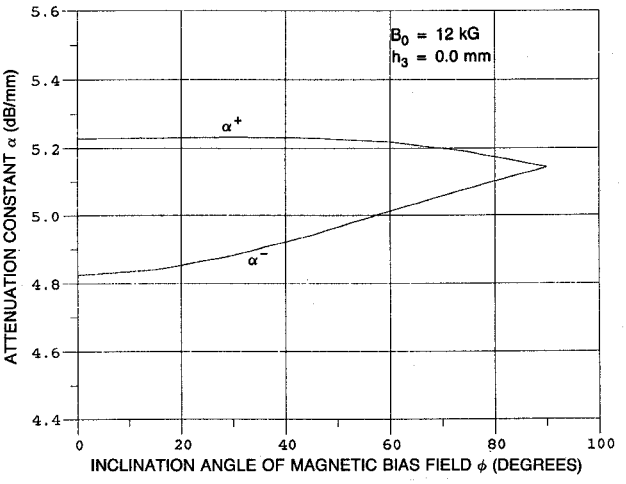

Fig. 6 Variation of α^+ and α^- with inclination angle ϕ.

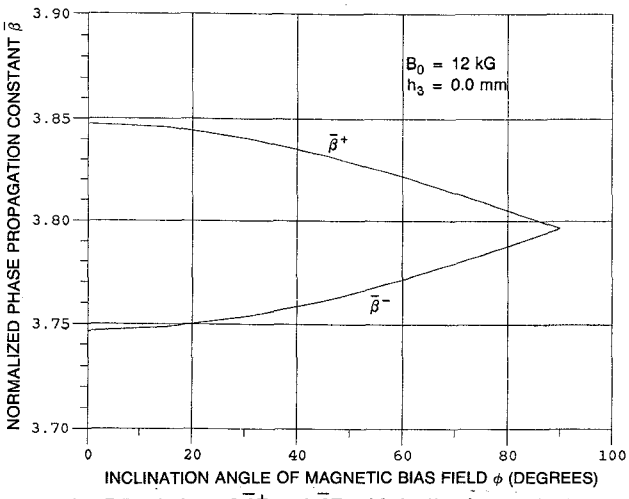

Fig. 7 Variation of $\bar{\beta}^+$ and $\bar{\beta}^-$ with inclination angle ϕ.

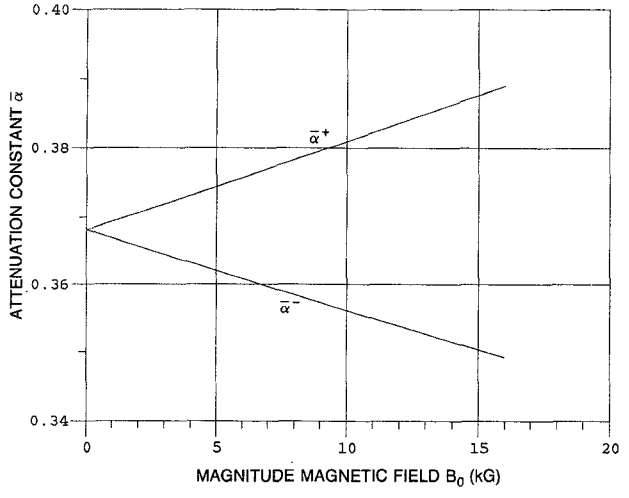

Fig. 8 Variation of $\bar{\alpha}^+$ and $\bar{\alpha}^-$ with magnetic field B_0. h_3 = 0.0 mm.

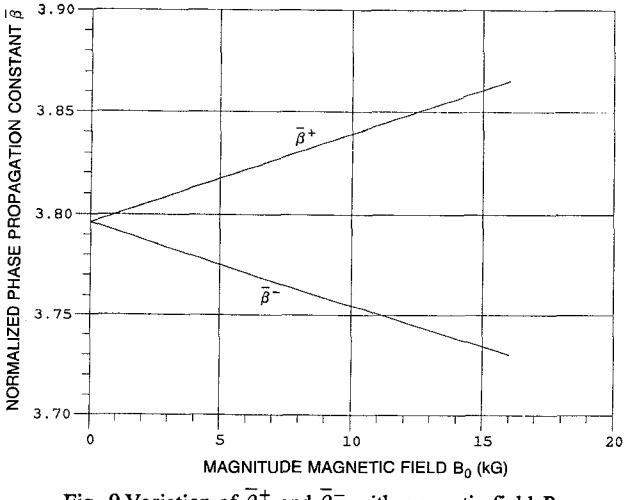

Fig. 9 Variation of $\bar{\beta}^+$ and $\bar{\beta}^-$ with magnetic field B_0. h_3 = 0.0 mm.

approach zero. A likely explanation for such a limiting characteristic is the creation of cyclotron electron orbits which are perpendicular to the B_0 direction and parallel to the planar interfaces. With $\phi = 0°$, Figs. 8 and 9 provide $\bar{\alpha}$ and $\bar{\beta}$, respectively, for varying B_0 up to 16 kG.

5. CONCLUSION

A full wave matrix spectral domain approach for complex anisotropy is used to find the propagation constants in the forward and reverse directions for suspended slot line layered structures. A dc bias magnetic field B_0 is employed to generate permittivity anisotropy in the semiconductor layer. The B_0 field is normal to the propagation direction, and its inclination angle ϕ to the interface is varied. Numerical results between 45 and 85 GHz for a GaAs semiconductor layer are obtained. Differences between forward and reverse attenuation constants (dB/λ_0) and phase constants (degrees/λ_0) show increases with increasing frequency. These differences appear to be largest, though, for small $\phi \lesssim 20°$.

6. REFERENCES

[1] B.R. McLeod and W.G. May, "A 35 GHz isolator using a coaxial solid-state plasma in a longitudinal magnetic field," IEEE Trans. Microwave Th. Tech., Vol., MTT-19, pp. 510-516, June 1971.

[2] A.V. Nurmikko, D.M. Bolle, and S. Talisa, "Guiding and control of millimeter waves by surface plasmon phenomena in semiconductors," Intern. J. Infrared Millimeter Waves, Vol., 1, pp. 3-13, 1980.

[3] D.M. Bolle and S.H. Talisa, "Fundamental considerations in millimeter and near-millimeter component design employing magnetoplasmons," IEEE Trans. Microwave Th. Tech., Vol., MTT-29, pp. 916-923, Sept. 1981.

[4] S.H. Talisa and D.M. Bolle, "Performance predictions for isolators and differential phase shifters for the near-millimeter wave range," IEEE Trans. Microwave Th. Tech., Vol. MTT-29, pp. 1338-1343, Dec. 1981.

[5] W-L. Hwang, S.H. Talisa, and D.M. Bolle, "New results for near-millimeter wave isolators and phase shifters based on magnetoplasmons on GaAs substrates," Intern. J. Infrared Millimeter Waves, Vol., 3, pp. 253-263, 1982.

[6] E.M. Godshalk and F.J. Rosenbaum, "Nonreciprocal effects in semiconductor loaded waveguide at millimeter wavelengths," IEEE Intern. Microwave Th. Tech. Symp. Dig., pp. 455-456, June 1984.

[7] C.M. Krowne, "Fourier transformed matrix method of finding propagation characteristics of complex anisotropic layered media," IEEE Trans. Microwave Th. Tech., Vol., MTT-32, pp. 1617-1625, Dec. 1984.

[8] A.A. Mostafa, C.M. Krowne, and K.A. Zaki, "Numerical spectral matrix method for propagation in general layered media: application to isotropic and anisotropic substrates," IEEE Trans. Microwave Th. Tech., Vol., MTT-35, pp. 1399-1407, Dec. 1987.